Published in final edited form as:

Hepatology. 2021 September ; 74(3): 1287–1299. doi:10.1002/hep.31822.

Increased adipose tissue fibrogenesis, not impaired expandability, is associated with nonalcoholic fatty liver disease

Joseph W. Beals[1], **Gordon I. Smith**[1], **Mahalakshmi Shankaran**[2], **Anja Fuchs**[3], **George G. Schweitzer**[1], **Jun Yoshino**[1], **Tyler Field**[2], **Marcy Matthews**[2], **Edna Nyangau**[2], **Darya Morozov**[4], **Bettina Mittendorfer**[1], **Marc K. Hellerstein**[2], **Samuel Klein**[1]

[1]Center for Human Nutrition and Atkins Center of Excellence in Obesity Medicine, Washington University School of Medicine, St Louis, MO.

[2]University of California Berkeley, Berkeley, CA.

[3]Department of Surgery, Washington University School of Medicine, St Louis, MO.

[4]Department of Radiology, Washington University School of Medicine, St Louis, MO.

Abstract

BACKGROUND AND AIMS: It is proposed that impaired expansion of subcutaneous adipose tissue (SAT) and an increase in adipose tissue fibrosis causes ectopic lipid accumulation, insulin resistance and metabolically unhealthy obesity. We therefore evaluated whether a decrease in SAT expandability, assessed by measuring SAT lipogenesis (triglyceride production), and an increase in SAT fibrogenesis (collagen production) are associated with NAFLD and insulin resistance in people with obesity.

APPROACH AND RESULTS: *In vivo* abdominal SAT lipogenesis and fibrogenesis, the expression of SAT genes involved in extracellular matrix (ECM) formation, and insulin sensitivity were assessed in three groups of participants stratified by adiposity and intrahepatic triglyceride (IHTG) content: 1) healthy lean with normal IHTG content (Lean-NL; n=12); 2) obese with normal IHTG content and normal glucose tolerance (Ob-NL; n=25); and 3) obese with NAFLD and abnormal glucose metabolism (Ob-NAFLD; n=25). Abdominal SAT triglyceride synthesis rates were greater (P <0.05) in both the Ob-NL (65.9±4.6 g/wk) and Ob-NAFLD (71.1±6.7 g/wk) than the Lean-NL group (16.2±2.8 g/wk) without a difference between the Ob-NL and Ob-NAFLD groups. Abdominal SAT collagen synthesis rate and the composite expression of genes encoding collagens progressively increased from the Lean-NL to the Ob-NL to the Ob-NAFLD groups and were greater in the Ob-NAFLD than the Ob-NL group (P <0.05). The composite expression of collagen genes was inversely correlated with both hepatic and whole-body insulin sensitivity (P <0.001).

Correspondence: Samuel Klein, MD, Center for Human Nutrition, Washington University School of Medicine, 660 S. Euclid Avenue, Campus Box 8031, St. Louis, MO 63110, USA, sklein@wustl.edu, telephone: 314-362-8708, FAX: 314-362-8230.

Author Contributions: J.W.B., G.I.S., and G.G.S. conducted the clinical studies, J.W.B., G.I.S., M.S., A.F., J.Y., T.F., M.M., E.N., and D.M. performed the sample and data analyses, M.K.H. and S.K. designed the study, J.W.B, G.I.S., B.M., M.K.H. and S.K. interpreted the data and wrote the manuscript. S.K. is the guarantor of this work and, as such, had full access to all the data in the study and takes responsibility for the integrity of the data and the accuracy of the data analysis. All authors critically reviewed and edited the manuscript.

ClinicalTrials.gov number: NCT02706262.

CONCLUSIONS: Adipose tissue expandability is not impaired in people with obesity and NAFLD. However, SAT fibrogenesis is greater in people with obesity and NAFLD than in those with obesity and normal IHTG content, and is inversely correlated with both hepatic and whole-body insulin sensitivity.

Keywords

obesity; lipogenesis; fibrosis; steatosis; insulin resistance

Nonalcoholic fatty liver disease (NAFLD) is a common complication of obesity and is typically associated with insulin-resistant glucose metabolism (1–4). It has been proposed that an inability to adequately increase subcutaneous adipose tissue (SAT) triglyceride (TG) stores in response to excess energy consumption and weight gain redirects lipids to other organs, such as the liver and skeletal muscle, leading to ectopic lipid accumulation and cellular lipotoxicity that causes insulin resistance in these organs (5–7). Adipose tissue fibrogenesis (i.e., collagen synthesis) is also important for adipose tissue expansion because it provides the structural framework needed to support the increase in adipose tissue mass. However, excessive adipose tissue extracellular matrix (ECM) formation and fibrosis have been proposed as an important cause of whole-body insulin resistance, because adipose tissue fibrosis is associated with insulin resistance in both rodents and people (8–10), whereas attenuating adipose tissue ECM formation prevents hepatic steatosis and insulin resistance in rodent models of obesity (6,10,11).

The potential importance of impaired SAT TG storage and SAT fibrogenesis in the pathogenesis of hepatic steatosis and insulin resistance in people with NAFLD is not known. Previous studies that evaluated SAT TG synthesis rates did not evaluate intrahepatic TG (IHTG) content or did not stratify study cohorts into those with and without NAFLD (12–14). Moreover, we are not aware of any studies that directly evaluated SAT collagen production rates in people. The purpose of the present study was to test the hypothesis that SAT TG synthesis (lipogenesis) is lower, whereas the rate of adipose tissue collagen synthesis (fibrogenesis) and regulators of fibrogenesis are higher in people with obesity and NAFLD than in people with obesity and normal IHTG content. To this end, we assessed *in vivo* rates of SAT TG and collagen synthesis by administering deuterated water (D_2O) daily for 3–5 weeks and measuring deuterium incorporation into the glycerol moiety of TG and collagen Iα1 in abdominal SAT in healthy lean participants and participants with obesity who were separated based on IHTG content and insulin-sensitive glucose metabolism. In addition, we measured: i) SAT expression of genes that are involved in ECM formation, namely those that encode for proteins involved in ECM production, macrophage markers and the nod-like receptor protein 3 (NLRP3) inflammasome (15–18); ii) plasma insulin concentrations over 24 hours because insulin is a regulator of collagen production (19–21); and iii) hepatic and whole-body insulin sensitivity assessed by using the hyperinsulinemic-euglycemic clamp procedure in conjunction with [U-^{13}C]labeled glucose tracer infusion.

Methods

Study participants

Sixty-two men and women participated in this study, which was conducted in the Clinical and Translational Research Unit (CTRU) at Washington University School of Medicine in St. Louis, MO from April 2016 to September 2019. Participant flow is shown in Supplemental Figure 1. Participants were recruited by using the Volunteers for Health database at Washington University School of Medicine and by advertising in the community. Written, informed consent was obtained from all participants before being enrolled in this study, which was approved by the Human Research Protection Office at Washington University School of Medicine in St. Louis, MO. All participants completed a comprehensive screening evaluation, including a medical history and physical examination, standard blood tests, hemoglobin A1c (HbA1c), an oral glucose tolerance test (OGTT), and assessment of IHTG content by using magnetic resonance imaging (MRI) to determine eligibility according to the following inclusion criteria: 1) metabolically healthy lean with normal IHTG content (Lean-NL) (n=12, 6 women) characterized bybody mass index (BMI) 18.5–24.9 kg/m^2, IHTG content <5%, plasma TG concentration <150 mg/dL, normal fasting plasma glucose (<100 mg/dL), normal oral glucose tolerance (plasma glucose <140 mg/dL 2 h after ingesting 75 g glucose) and HbA1c (≤5.6%); 2) obese with normal IHTG content and normal glucose tolerance (Ob-NL (n=25, 3 men) characterized by BMI 30.0–49.9 kg/m^2, IHTG content <5%, plasma TG concentration <150 mg/dL, normal fasting plasma glucose, oral glucose tolerance, and HbA1c; and 3) obese with NAFLD and abnormal glucose metabolism (Ob-NAFLD) (n=25, 3 men) characterized by BMI 30.0–49.9 kg/m^2, IHTG content ≥7% and abnormal glucose metabolism determined by HbA1c 5.7%−6.4%, fasting plasma glucose 100–125 mg/dL, or 2-hr OGTT plasma glucose concentration 140–199 mg/dL. Potential participants who had a history of diabetes or liver disease other than NAFLD, consumed excessive amounts of alcohol (>21 units per week for men and >14 units per week for women), were taking medications that could affect the study outcome measures, were pregnant or lactating, or had metal implants that precluded MRI were excluded from the study.

Body composition analyses

Body fat mass and fat-free mass (FFM) were determined by using dual-energy X-ray absorptiometry (Lunar iDXA, GE, Madison, WI). Abdominal SAT and intra-abdominal adipose tissue (IAAT) volumes and IHTG content were determined using MRI (3-T superconducting magnet; Siemens, Iselin, NJ).

D_2O labeling protocol and abdominal SAT biopsy procedure

Subjects consumed 50-mL aliquots of 70% D_2O (Sigma-Aldrich, St. Louis, MO), provided in sterile vials, 3–4 times daily for 5 days (priming period) and then daily for 3–5 weeks. The final aliquot was consumed on the evening before the adipose tissue biopsy was obtained. Compliance with D_2O consumption was monitored by interview at weekly visits to the CTRU, by counting the empty vials returned at each visit, and by evaluating D_2O enrichments in plasma (obtained weekly) and saliva (obtained on days 2, 4, and 11 and weekly thereafter). At the end of the labeling period, ~2 g of abdominal SAT was obtained

by manual aspiration with a 4-mm liposuction cannula and rinsed with ice-cold saline and immediately frozen in liquid nitrogen and stored at −80°C for later analysis. In a representative participant from each of the three groups (Lean-NL, Ob-NL and Ob-NAFLD), subcutaneous adipose tissue samples were also fixed in formalin and embedded in paraffin. Paraffin sections were stained with Masson's trichrome for collagen and images were acquired at 40x magnification by using a Nikon Coolscope microscope (Nikon, Japan).

Integrated 24-h plasma insulin concentration and assessment of insulin sensitivity

Participants were admitted to the CTRU at 1800 h for ~48 hours for metabolic testing. Participants consumed a standard meal (50% carbohydrate, 35% fat, 15% protein) containing one-third of their estimated energy requirements (22) between 1800 h and 1900 h on the day of admission and then fasted until the next morning (day 2). At 0630 h on day 2, a catheter was inserted into an antecubital vein for 24-h serial blood sampling. Blood samples were obtained hourly from 0700 h to 2300 h on day 2 and from 0500 h to 0700 h on day 3; additional blood samples were obtained at 30 min and 90 min after each meal, which were given at 0700 h, 1300 h, and 1900 h. Each meal contained one-third of the participant's estimated energy requirement (22) and provided 50% of energy as carbohydrates, 35% as fat and 15% as protein. After the evening meal was consumed on day 2, participants fasted until the end of the hyperinsulinemic-euglycemic clamp procedure conducted on day 3. At 0700 h on day 3, a primed (8.0 μmol/kg) continuous (0.08 μmol/kg/min) infusion of [U-^{13}C]glucose (Cambridge Isotope Laboratories Inc., Andover, MA) was started through the existing intravenous catheter. An additional catheter was inserted into a radial artery to obtain arterial blood samples. After the infusion of glucose tracer for 210 min (basal period), insulin was infused for 210 min at a rate of 50 mU/m^2 body surface area [BSA]/min (initiated with a two-step priming dose of 200 mU/m^2 BSA/min for 5 min followed by 100 mU/m^2 BSA/min for 5 min). The infusion of [U-^{13}C]glucose was stopped during insulin infusion because of the expected decrease in hepatic glucose production (23). Euglycemia (~100 mg/dL) was maintained by variable infusion of 20% dextrose enriched to ~1% with [U-^{13}C]glucose. Blood samples were obtained before beginning the tracer infusion and every 6–7 minutes during the final 20 minutes of the basal and insulin infusion periods. Due to technical issues, one participant in the Ob-NL and one in the Ob-NAFLD group did not complete the 24-h blood sampling protocol; two participants in the Ob-NL and one in the Ob-NAFLD group did not complete the clamp procedure.

Plasma substrate and insulin concentrations

Plasma glucose concentration was determined by using an automated glucose analyzer (Yellow Spring Instruments Co.). Fasting plasma insulin, hemoglobin A1c (HbA1c), lipid profile, and liver biochemistries were determined by using an automated chemistry analyzer (cobas 6000, Roche Diagnostics) in the Washington University Core Laboratory for Clinical Studies.

Adipose tissue dynamics and plasma glucose kinetics

Deuterium enrichment in plasma and saliva samples and [U-^{13}C]glucose enrichment in plasma glucose were determined by using gas-chromatography/mass-spectrometry (GC-MS) (12,24). To determine the deuterium enrichment and labeling pattern of TG-glycerol

in SAT, lipids were extracted from adipose tissue and TG-glycerol was converted to glycerol triacetate before GC-MS analysis (25). Deuterium enrichment in collagen Iα1 of adipose tissue was determined after extraction and trypsin digestion followed by liquid chromatography tandem mass spectrometry analysis (26).

Adipose tissue RNA sequencing

Total RNA was isolated from frozen SAT samples by using QIAzol and an RNeasy mini kit in combination with an RNase-free DNase Set (Qiagen, Valencia, CA)(27). Four samples from the Ob-NL group, and one from the Ob-NAFLD group were excluded from further analysis due to poor RNA quality or quantity. Library preparation of the remaining samples was performed with mRNA reverse transcribed to yield cDNA fragments, which were then sequenced by using an Illumina NovaSeq 6000 at the UC San Diego IGM Genomics Center. Gene expression of cluster of differentiation 68 (*CD68*), connective tissue growth factor (*CTGF*), lysyl oxidase (*LOX*), lysyl oxidase-like protein 1 (*LOXL1*), lysyl oxidase-like protein 2 (*LOXL2*), mannose receptor C-type 1 (*MRC1*), nod-like receptor protein 3 (*NLRP3*), platelet-derived growth factor subunit A (*PDGFA).* secreted protein acidic and cysteine rich (*SPARC*), transforming growth factor beta-1 proprotein (*TGFB1*), and tenomodulin (*TNMD*) was identified as counts per million (CPM) reads and $\log_2$-transformed prior to analysis. The RNA sequencing data have been deposited in the Gene Expression Omnibus database, https://www.ncbi.nlm.nih.gov/geo (accession no. GSE159924).

Calculations

Plasma insulin 24-h area-under-the-curve (AUC) was calculated by using the trapezoidal method (28). The hepatic insulin sensitivity index (HISI) was calculated as the inverse of the product of plasma insulin concentration and endogenous glucose rate of appearance (Ra) into the systemic circulation during the last 20 minutes of the basal period of the clamp procedure (2). Insulin-stimulated glucose rate of disposal was determined during the last 20 minutes of the clamp procedure (2). Mass isotopomer distribution analysis was used to determine the fractional synthesis rates (FSR) of abdominal SAT TG and collagen (25). Total abdominal SAT TG synthesis rate was calculated as the product of the TG FSR and abdominal SAT mass, assuming adipose tissue density is 0.9196 (29). Composite collagen gene expression values were calculated as the average expression of collagens *1A1, 1A2, 3A1, 5A1, 5A2, 5A3, 6A1, 6A2, 6A3, 12A1, 14A1, and 24A1* after converting expression of each isoform to a *Z*-distribution.

Statistical Analysis

One-way analysis of variance (ANOVA) was performed to determine if participant characteristics and outcome measures were different between the Lean-NL, Ob-NL and Ob-NAFLD groups; Fisher's least significant difference procedure was used to locate significant mean differences when appropriate. In addition, polynomial contrasts were performed to describe the linear trend from the Lean-NL to the Ob-NL to the Ob-NAFLD group. In addition, relationships between outcome measures and metabolic variables were evaluated by using linear and nonlinear regression analysis with the best-fit to the data reported. A *P*-value ≤0.05 was considered statistically significant. Data are reported as means ± SEM

unless otherwise noted. Statistical analyses were performed by using SPSS (version 25, IBM, Armonk, NY). Based on a previous report that evaluated SAT TG FSR in insulin-resistant and insulin sensitive people with obesity (12), we estimated that 25 participants in each obese group would be needed to detect a 0.25 %/wk difference in the TG FSR with a two-sided α value of 0.05 and a power of 0.8.

Results

Participant characteristics

Body mass index, percent body fat, and abdominal SAT volume were not different between the Ob-NL and Ob-NAFLD groups but were greater in the obese groups than the Lean-NL group (Table 1). IAAT volume and IHTG content were greater in the Ob-NAFLD than in the Ob-NL group. The volume of IAAT was also greater in the Ob-NL than the Lean-NL group, whereas IHTG content was not different between the Ob-NL and Lean-NL groups. Fasting plasma glucose and TG concentrations, 2-h plasma glucose concentration during the OGTT, HbA1c and the 24-h plasma glucose concentration AUC were greater in the Ob-NAFLD than in the Lean-NL and Ob-NL groups, which were not different from each other. Fasting plasma insulin and integrated 24-h insulin concentrations progressively increased, whereas plasma HDL-cholesterol concentration and hepatic and whole-body insulin sensitivity progressively decreased from the Lean-NL to the Ob-NL to the Ob-NAFLD group.

Subcutaneous adipose tissue triglyceride synthesis is increased in people with obesity

Mean body water deuterium enrichment, assessed throughout D_2O administration, was not different among the Lean-NL, Ob-NL and Ob-NAFLD groups (1.51 ± 0.11, 1.41 ± 0.06, and 1.49 ± 0.06 %, respectively; P=0.61). Mean TG FSR in abdominal SAT was not different among groups (P=0.54; Figure 1A), however, total abdominal SAT TG synthesis rate was ~4-fold greater in the Ob-NL and Ob-NAFLD groups than in the Lean-NL group in proportion to the greater abdominal SAT volume in both obese groups than in the lean group (P<0.05; Figure 1B).

Fibrogenesis in SAT is increased in people with obesity and NAFLD

Collagen accumulation in abdominal SAT, assessed by Masson's trichrome stain in representative participants, was greater in the Ob-NAFLD than in the Lean-NL and Ob-NL groups (Figure 2A). Collagen Iα1 FSR increased progressively from the Lean-NL to the Ob-NL to the Ob-NAFLD group (Linear trend P <0.001) and was greater in the Ob-NAFLD group than in the Lean-NL and Ob-NL groups (Figure 2B). The composite expression of genes encoding 12 collagen isoforms progressively increased from the Lean-NL to the Ob-NL to the Ob-NAFLD group (Linear trend P <0.001) and was greater in the Ob-NAFLD than the Ob-NL group (Figure 2C and Supplementary Figure 2).

Consistent with these findings, we found adipose tissue expression of key regulators of adipose tissue ECM formation (*SPARC*, *CTGF*, *TNMD*, *PDGFA, TGFB1, LOX*, *LOXL1,* and *LOXL2*) increased progressively from the Lean-NL to the Ob-NL to the Ob-NAFLD group (Linear trend P <0.001) and was significantly greater in the Ob-NAFLD than the Ob-NL group for *SPARC*, *TNMD*, *LOX*, and *LOXL1* (Figure 2D). Moreover, SAT expression

of these genes were positively correlated with the composite of collagen gene expression (Figure 3).

Macrophage markers and the NLRP3 inflammasome are increased in people with obesity and NAFLD and are directly associated with fibrogenesis

We found SAT gene expression of macrophage markers *CD68* and *MRC1* and gene expression of *NLRP3* progressively increased from the Lean-NL to Ob-NL to the Ob-NAFLD group (Linear trend $P<0.001$), were greater in both obese groups than the Lean-NL group, and were greater in the Ob-NAFLD than the Ob-NL group (Figure 4A). In addition, SAT gene expression of *CD68*, *MRC1* and *NLRP3* correlated directly with the composite expression of collagen genes in SAT (Figure 4B).

Fibrogenesis is positively correlated with circulating insulin and inversely correlated with insulin sensitivity

The production of collagen and secreted protein acidic and cysteine rich (SPARC), which is a major nonstructural protein of the ECM, are regulated by insulin (19–21). We found a significant positive correlation between the 24-h plasma insulin concentration AUC and SAT expression of both collagen and *SPARC* (Figure 5A). In addition, the composite collagen gene expression was inversely correlated with both hepatic and whole-body insulin sensitivity (Figure 5B)

Discussion

In the present study we evaluated whether impaired SAT expandability (assessed as SAT TG synthesis) and adipose tissue fibrogenesis are associated with increased IHTG content and insulin resistant-glucose metabolism in people with obesity. We found total SAT TG synthesis rate was greater in both the Ob-NL and Ob-NALFD groups than in the Lean-NL group, without a difference between the two obese groups. However, SAT collagen synthesis rate and the composite expression of collagen genes progressively increased from the Lean-NL to the Ob-NL to the Ob-NALFD group, and were greater in the Ob-NL than the Lean-NL group and greater in the Ob-NAFLD than the Ob-NL group. In addition, the expression of collagen genes was inversely correlated with hepatic and whole-body insulin sensitivity. Taken together, these data suggest impaired adipose tissue expandability is not responsible for ectopic fat accumulation or insulin resistance in people with obesity, but instead demonstrate a link between adipose tissue fibrogenesis and insulin resistance. Moreover, the composite of SAT collagen gene expression correlated with systemic 24-h insulin concentrations and with SAT expression of factors that regulate ECM formation, suggesting a complex integration of systemic and local stimuli contribute to increased adipose tissue fibrogenesis in people with obesity.

The ECM, which is comprised of structural proteins, adhesion proteins and proteoglycans, provides structural support for adipocytes. Increased ECM formation and remodeling are required during adipose tissue expansion in response to prolonged periods of positive energy balance to support the increase in adipose tissue mass (30,31). Previous studies have shown that SAT expression of genes that encode for components of the ECM are greater in people

with obesity than in those who are lean (8,32,33). Our data are consistent with these findings, but also demonstrate there are significant differences in SAT ECM biology among people with obesity based on their metabolic health and IHTG content that are independent of adiposity *per se*. Moreover, the expression of SAT genes involved in the production of collagen and other ECM components and the FSR of collagen in SAT were also greater in the Ob-NAFLD than the Ob-NL group, even though both groups were matched on body fat mass.

The results from the present study and those from previous studies suggest several mechanisms might be responsible for the increase in SAT fibrogenesis in the Ob-NAFLD group. First, the higher plasma insulin concentrations in the Ob-NAFLD than the Ob-NL group could have contributed to the differences in collagen production observed between the two groups. Mean 24-hour plasma insulin AUC in the Ob-NAFLD group was double the value in the Ob-NL group and expression of genes that encode for collagen and SPARC were positively associated with 24-hour plasma insulin AUC values. The importance of insulin in regulating ECM production has been demonstrated in studies conducted in cell culture systems that found collagen production and both gene and protein expression of SPARC are regulated by insulin (19–21,34). Moreover, chronic insulin administration increases AT fibrosis in wild-type mice whereas, streptozotocin treatment to reduce insulin secretion alleviates AT fibrosis in rodent models of obesity (35). Second, we found the expression of macrophage markers in SAT positively correlated with the composite expression of collagen. Adipose tissue macrophages are involved in adipose tissue fibrogenesis by producing collagen and by releasing soluble mediators that stimulate the production of ECM components by other cells, such as myofibroblasts, adipose tissue progenitor cells and committed preadipocytes (15,36). Third, the positive correlation between SAT gene expression of NLRP3 and the composite expression of collagen support the possibility that the NLRP3 inflammasome contributes to adipose tissue fibrosis in people with obesity. Increased NLRP3 inflammasome activity is associated with increased markers of adipose tissue fibrosis in people with the metabolic syndrome (37), obesity with type 2 diabetes and obesity with NAFLD (17). Furthermore, blocking NLRP3 activity in adipocytes obtained from people with obesity reduces the expression of collagen genes (17). Finally, data from previous studies have shown decreased adipose tissue oxygen tension contributes to adipose tissue inflammation and increased fibrogenesis in obesity. Hypoxia inducible factor-1α (HIF-1α), a transcription factor that responds to low oxygen tension, increases adipose tissue gene expression of multiple ECM components (11,38). Studies conducted in obese rodent models (11,18,39) and in people with obesity (9,17,40) have shown adipose tissue hypoxia increases inflammation and is associated with increased adipose tissue expression of genes that encode ECM proteins. Together, the results from the present and previous studies suggest multiple factors, including increased circulating insulin, increased adipose tissue inflammation, and decreased adipose tissue oxygen tension are involved in stimulating adipose tissue fibrogenesis and ECM remodeling in people with obesity.

The participants in our study had a large range in values for both hepatic and whole-body insulin sensitivity, determined by using the hyperinsulinemic-euglycemic clamp procedure. Adipose tissue composite of collagen gene expression was inversely associated with hepatic and whole-body insulin sensitivity. These data are consistent with and extend previous

studies that have shown adipose tissue fibrosis and the expression of genes involved in regulating ECM production are associated with insulin-resistant glucose metabolism (8,15,17,35,40,41). In rodent models of obesity, increased adipose tissue fibrogenesis and fibrosis can cause whole-body insulin resistance (6), whereas pharmacologic or genetic disruption of ECM production improves insulin sensitivity (6,10,11). Moreover, adipose tissue expression of SPARC, which was greater in our Ob-NAFLD than Ob-NL participants, increases adipose tissue production of plasminogen activator inhibitor-1 (PAI-1) (34). Overexpression of adipose tissue PAI-1 causes whole-body insulin resistance in rodents (42) and plasma PAI-1 concentration is inversely correlated with whole-body insulin sensitivity in people with obesity (43). These observations suggest a feed-forward cycle, in which a sustained increase in circulating insulin drives adipose tissue ECM formation/fibrosis, which in turn may exacerbate insulin resistance and lead to a further increase in circulating insulin.

Our data do not support the notion that an inability to expand adipose tissue mass in people with obesity and NAFLD is involved in the pathogenesis of hepatic steatosis. The rates of TG synthesis in SAT were greater in both the Ob-NL and Ob-NAFLD groups than in the Lean-NL group, but were not different between the Ob-NL and Ob-NAFLD groups. Moreover, based on an assumed liver mass of 1.75 kg in people with obesity (44), the estimated amount of IHTG in the Ob-NAFLD group was <1% of total body TG mass. Therefore, it is improbable that this small amount of IHTG could not be accommodated by body SAT depots. Instead, hepatic steatosis in people with NAFLD is more likely caused by alterations in liver physiology, including increased hepatic *de novo* lipogenesis and hepatic fatty acid uptake (45–49).

In conclusion, rates of adipose tissue TG synthesis in people with obesity and NAFLD were not different than observed in people with obesity who were matched on adiposity but had normal IHTG content. This finding is inconsistent with the concept that hepatic lipid accumulation is driven by impaired adipose tissue expandability. However, rates of collagen synthesis and composite expression of collagen genes in SAT were greater in the Ob-NAFLD than in the Ob-NL group and were inversely correlated with hepatic and whole body insulin sensitivity, demonstrating alterations in adipose tissue ECM metabolism are associated with insulin resistance but are independent of fat mass *per se*. Although the mechanisms responsible for the increase in SAT fibrogenesis in the Ob-NL and further increase in the Ob-NAFLD group are not clear, our data suggest that systemic hyperinsulinemia and activation of specific components of the adipose tissue immune system, namely the NLRP3 inflammasome and macrophages, are involved in this process.

Supplementary Material

Refer to Web version on PubMed Central for supplementary material.

Acknowledgements

The authors thank Jennifer Shew, Frieda Custodio and Dr. Adewole Okunade for their technical assistance, Janet Winkelmann, Sally Torbitzky and the nurses of the Clinical and Translational Research Unit for their assistance in conducting the studies, and the study subjects for their participation.

Grant Support: This study was supported by National Institutes of Health grants P30 DK56341 (Nutrition Obesity Research Center), P30 DK052574 (Digestive Disease Research Center), UL1 TR002345 (Clinical and Translational Science Award), S10 OD026929 (UC San Diego IGM Genomics Center) and T32 HL130357, and funding from the College of Natural Resources of the University of California Berkeley and the Centene Corporation contract (P19–00559) for the Washington University-Centene ARCH Personalized Medicine Initiative.

Conflicts of Interest: S.K. receives research funding from Janssen Pharmaceuticals and serves on a Scientific Advisory Board for Merck Sharp & Dohme Corp. and Altimmune. M.K.H. receives research funding from Gilead Sciences Inc., Merck Sharp & Dohme Corp., and Pfizer Inc. The other authors have nothing to disclose.

Abbreviations:

ALT	alanine aminotransferase
AST	aspartate aminotransferase
BMI	body mass index
CD68	cluster of differentiation 68
CPM	counts per million
CTGF	connective tissue growth factor
CTRU	Clinical and Translational Research Unit
ECM	extracellular matrix
FFM	fat-free mass
FSR	fractional synthesis rate
GC-MS	gas-chromatography/mass-spectrometry
HbA1c	hemoglobin A1c
HIF-1α	hypoxia inducible factor-1α
HISI	hepatic insulin sensitivity index
IAAT	intraabdominal adipose tissue
IHTG	intrahepatic triglyceride
LOX	lysyl oxidase
LOXL1	lysyl oxidase-like protein 1
LOXL2	lysyl oxidase-like protein 2
MRC1	mannose receptor C-type 1
MRI	magnetic resonance imaging
NL	normal
NLRP3	nod-like receptor protein 3

Ob	obese
OGTT	oral glucose tolerance test
PAI-1	plasminogen activator inhibitor-1
PDGFA	Platelet-derived growth factor subunit A
Ra	rate of appearance
SAT	subcutaneous adipose tissue
SPARC	secreted protein acidic and cysteine rich
TG	triglyceride
TGFB1	transforming growth factor beta-1 proprotein
TNMD	tenomodulin

REFERENCES

1. Ter Horst KW, Gilijamse PW, Versteeg RI, Ackermans MT, Nederveen AJ, la Fleur SE, et al. Hepatic diacylglycerol-associated protein kinase Cε translocation links hepatic steatosis to hepatic insulin resistance in humans. Cell Rep. 2017;19:1997–2004. [PubMed: 28591572]
2. Korenblat KM, Fabbrini E, Mohammed BS, Klein S. Liver, muscle, and adipose tissue insulin action is directly related to intrahepatic triglyceride content in obese subjects. Gastroenterology. 2008;134:1369–1375. [PubMed: 18355813]
3. Sanyal AJ, Campbell–Sargent C, Mirshahi F, Rizzo WB, Contos MJ, Sterling RK, et al. Nonalcoholic steatohepatitis: Association of insulin resistance and mitochondrial abnormalities. Gastroenterology. 2001;120:1183–1192. [PubMed: 11266382]
4. Sharpton SR, Schnabl B, Knight R, Loomba R. Current Concepts, Opportunities, and Challenges of Gut Microbiome-Based Personalized Medicine in Nonalcoholic Fatty Liver Disease. Cell Metab. 2021;33:21–32. [PubMed: 33296678]
5. Virtue S, Vidal-Puig A. Adipose tissue expandability, lipotoxicity and the Metabolic Syndrome--an allostatic perspective. Biochim. Biophys. Acta. 2010;1801:338–349. [PubMed: 20056169]
6. Sun K, Park J, Gupta OT, Holland WL, Auerbach P, Zhang N, et al. Endotrophin triggers adipose tissue fibrosis and metabolic dysfunction. Nat. Commun. 2014;5:3485. [PubMed: 24647224]
7. Vishvanath L, Gupta RK. Contribution of adipogenesis to healthy adipose tissue expansion in obesity. J. Clin. Invest. 2019;129:4022–4031. [PubMed: 31573549]
8. Yoshino J, Patterson BW, Klein S. Adipose tissue CTGF expression is associated with adiposity and insulin resistance in humans. Obesity. 2019;27:957–962. [PubMed: 31004409]
9. Cifarelli V, Beeman SC, Smith GI, Yoshino J, Morozov D, Beals JW, et al. . Decreased adipose tissue oxygenation associates with insulin resistance in individuals with obesity. J. Clin. Invest. 2020;130.
10. Khan T, Muise ES, Iyengar P, Wang ZV, Chandalia M, Abate N, et al. Metabolic dysregulation and adipose tissue fibrosis: role of collagen VI. Mol. Cell. Biol. 2009;29:1575–1591. [PubMed: 19114551]
11. Halberg N, Khan T, Trujillo ME, Wernstedt-Asterholm I, Attie AD, Sherwani S, et al. Hypoxia-inducible factor 1α induces fibrosis and insulin resistance in white adipose tissue. Mol. Cell. Biol. 2009;29:4467–4483. [PubMed: 19546236]
12. Nouws J, Fitch M, Mata M, Santoro N, Galuppo B, Kursawe R, et al. Altered in vivo lipid fluxes and cell dynamics in subcutaneous adipose tissues are associated with the unfavorable pattern of fat distribution in obese adolescent girls. Diabetes. 2019;68:1168–1177. [PubMed: 30936147]

13. Allister CA, Liu L, Lamendola CA, Craig CM, Cushman SW, Hellerstein MK, et al. In vivo 2H2O administration reveals impaired triglyceride storage in adipose tissue of insulin-resistant humans. J. Lipid Res. 2015;56:435–439. [PubMed: 25418322]
14. Tuvdendorj D, Chandalia M, Batbayar T, Saraf M, Beysen C, Murphy EJ, et al. Altered subcutaneous abdominal adipose tissue lipid synthesis in obese, insulin-resistant humans. Am. J. Physiol. - Endocrinol. Metab. 2013;305:E999–E1006. [PubMed: 23982159]
15. Sun K, Tordjman J, Clément K, Scherer PE. Fibrosis and adipose tissue dysfunction. Cell Metab. 2013;18:470–477. [PubMed: 23954640]
16. Ouyang X, Ghani A, Mehal WZ. Inflammasome biology in fibrogenesis. Biochim. Biophys. Acta - Mol. Basis Dis. 2013;1832:979–988.
17. Unamuno X, Gómez-Ambrosi J, Ramírez B, Rodríguez A, Becerril S, Valentí V, et al. NLRP3 inflammasome blockade reduces adipose tissue inflammation and extracellular matrix remodeling. Cell. Mol. Immunol. 2019;1–13.
18. Kumar D, Pandya SK, Varshney S, Shankar K, Rajan S, Srivastava A, et al. . Temporal immmunometabolic profiling of adipose tissue in HFD-induced obesity: manifestations of mast cells in fibrosis and senescence. Int. J. Obes. 2019;43:1281–1294.
19. Kos K, Wong S, Tan B, Gummesson A, Jernas M, Franck N, et al. Regulation of the fibrosis and angiogenesis promoter SPARC/osteonectin in human adipose tissue by weight change, leptin, insulin, and glucose. Diabetes. 2009;58:1780–1788. [PubMed: 19509023]
20. Goldstein RH, Poliks CF, Pilch PF, Smith BD, Fine A. Stimulation of collagen formation by insulin and insulin-like growth factor I in cultures of human lung fibroblasts. Endocrinology. 1989;124:964–970. [PubMed: 2463909]
21. Wang P, Keijer J, Bunschoten A, Bouwman F, Renes J, Mariman E. Insulin modulates the secretion of proteins from mature 3T3-L1 adipocytes: a role for transcriptional regulation of processing. Diabetologia. 2006;49:2453–2462. [PubMed: 16896944]
22. Mifflin MD, St Jeor ST, Hill LA, Scott BJ, Daugherty SA, Koh YO. A new predictive equation for resting energy expenditure in healthy individuals. Am. J. Clin. Nutr. 1990;51:241–247. [PubMed: 2305711]
23. Klein S, Fontana L, Young VL, Coggan AR, Kilo C, Patterson BW, et al. Absence of an effect of liposuction on insulin action and risk factors for coronary heart disease. N. Engl. J. Med. 2004;350:2549–2557. [PubMed: 15201411]
24. Mittendorfer B, Horowitz JF, Klein S. Gender differences in lipid and glucose kinetics during short-term fasting. Am. J. Physiol.-Endocrinol. Metab. 2001;281:E1333–E1339. [PubMed: 11701450]
25. Turner SM, Murphy EJ, Neese RA, Antelo F, Thomas T, Agarwal A, et al. Measurement of TG synthesis and turnover in vivo by 2H2O incorporation into the glycerol moiety and application of MIDA. Am. J. Physiol.-Endocrinol. Metab. 2003;285:E790–E803. [PubMed: 12824084]
26. Decaris ML, Li KW, Emson CL, Gatmaitan M, Liu S, Wang Y, et al. Identifying nonalcoholic fatty liver disease patients with active fibrosis by measuring extracellular matrix remodeling rates in tissue and blood. Hepatology. 2017;65:78–88. [PubMed: 27706836]
27. Yamaguchi S, Franczyk MP, Chondronikola M, Qi N, Gunawardana SC, Stromsdorfer KL, et al. Adipose tissue NAD+ biosynthesis is required for regulating adaptive thermogenesis and whole-body energy homeostasis in mice. Proc. Natl. Acad. Sci. U. S. A. 2019;116:23822–23828. [PubMed: 31694884]
28. Allison DB, Paultre F, Maggio C, Mezzitis N, Pi-Sunyer FX. The use of areas under curves in diabetes research. Diabetes Care. 1995;18:245–250. [PubMed: 7729306]
29. Abate N, Burns D, Peshock RM, Garg A, Grundy SM. Estimation of adipose tissue mass by magnetic resonance imaging: validation against dissection in human cadavers. J. Lipid Res. 1994;35:1490–1496. [PubMed: 7989873]
30. Mariman ECM, Wang P. Adipocyte extracellular matrix composition, dynamics and role in obesity. Cell. Mol. Life Sci. 2010;67:1277–1292. [PubMed: 20107860]
31. Chun T-H, Hotary KB, Sabeh F, Saltiel AR, Allen ED, Weiss SJ. A pericellular collagenase directs the 3-dimensional development of white adipose tissue. Cell. 2006;125:577–591. [PubMed: 16678100]

32. Pasarica M, Gowronska-Kozak B, Burk D, Remedios I, Hymel D, Gimble J, et al. Adipose tissue collagen VI in obesity. J. Clin. Endocrinol. Metab. 2009;94:5155–5162. [PubMed: 19837927]
33. Spencer M, Unal R, Zhu B, Rasouli N, McGehee RE, Peterson CA, et al. . Adipose tissue extracellular matrix and vascular abnormalities in obesity and insulin resistance. J. Clin. Endocrinol. Metab. 2011;96:E1990–1998. [PubMed: 21994960]
34. Tartare-Deckert S, Chavey C, Monthouel M-N, Gautier N, Obberghen EV. The matricellular protein SPARC/osteonectin as a newly identified factor up-regulated in obesity. J. Biol. Chem. 2001;276:22231–22237. [PubMed: 11294850]
35. Kumar D, Shankar K, Patel S, Gupta A, Varshney S, Gupta S, et al. Chronic hyperinsulinemia promotes meta-inflammation and extracellular matrix deposition in adipose tissue: Implications of nitric oxide. Mol. Cell. Endocrinol. 2018;477:15–28. [PubMed: 29753026]
36. Marcelin G, Silveira ALM, Martins LB, Ferreira AV, Clément K. Deciphering the cellular interplays underlying obesity-induced adipose tissue fibrosis. J. Clin. Invest. 2019;129:4032–4040. [PubMed: 31498150]
37. Pahwa R, Singh A, Adams-Huet B, Devaraj S, Jialal I. Increased inflammasome activity in subcutaneous adipose tissue of patients with metabolic syndrome. Diabetes Metab. Res. Rev. 2020;e3383. [PubMed: 32652811]
38. Li X, Li J, Wang L, Li A, Qiu Z, Qi L, et al. The role of metformin and resveratrol in the prevention of hypoxia-inducible factor 1α accumulation and fibrosis in hypoxic adipose tissue. Br. J. Pharmacol. 2016;173:2001–2015. [PubMed: 27059094]
39. Seo JB, Riopel M, Cabrales P, Huh JY, Bandyopadhyay GK, Andreyev AYu, et al. Knockdown of ANT2 reduces adipocyte hypoxia and improves insulin resistance in obesity. Nat. Metab. 2019;1:86–97. [PubMed: 31528845]
40. Lawler HM, Underkofler CM, Kern PA, Erickson C, Bredbeck B, Rasouli N. Adipose tissue hypoxia, inflammation, and fibrosis in obese insulin-sensitive and obese insulin-resistant subjects. J. Clin. Endocrinol. Metab. 2016;101:1422–1428. [PubMed: 26871994]
41. Dankel SN, Svärd J, Matthä S, Claussnitzer M, Klöting N, Glunk V, et al. COL6A3 expression in adipocytes associates with insulin resistance and depends on PPARγ and adipocyte size. Obesity. 2014;22:1807–1813. [PubMed: 24719315]
42. Lijnen HR, Alessi M-C, Van Hoef B, Collen D, Juhan-Vague I. On the role of plasminogen activator inhibitor-1 in adipose tissue development and insulin resistance in mice. J. Thromb. Haemost. 2005;3:1174–1179. [PubMed: 15946208]
43. Potter van Loon BJ, Kluft C, Radder JK, Blankenstein MA, Meinders AE. The cardiovascular risk factor plasminogen activator inhibitor type 1 is related to insulin resistance. Metabolism. 1993;42:945–949. [PubMed: 8345817]
44. Bosy-Westphal A, Kossel E, Goele K, Later W, Hitze B, Settler U, et al. Contribution of individual organ mass loss to weight loss–associated decline in resting energy expenditure. Am. J. Clin. Nutr. 2009;90:993–1001. [PubMed: 19710198]
45. Smith GI, Shankaran M, Yoshino M, Schweitzer GG, Chondronikola M, Beals JW, et al. Insulin resistance drives hepatic de novo lipogenesis in nonalcoholic fatty liver disease. J. Clin. Invest. 2020;130:1453–1460. [PubMed: 31805015]
46. Greco D, Kotronen A, Westerbacka J, Puig O, Arkkila P, Kiviluoto T, et al. Gene expression in human NAFLD. Am. J. Physiol. Gastrointest. Liver Physiol. 2008;294:G1281–1287. [PubMed: 18388185]
47. Lambert JE, Ramos-Roman MA, Browning JD, Parks EJ. Increased de novo lipogenesis is a distinct characteristic of individuals with nonalcoholic fatty liver disease. Gastroenterology. 2014;146:726–735. [PubMed: 24316260]
48. Khan RS, Bril F, Cusi K, Newsome PN. Modulation of insulin resistance in nonalcoholic fatty liver disease. Hepatology. 2019;70:711–724. [PubMed: 30556145]
49. Cohen JC, Horton JD, Hobbs HH. Human fatty liver disease: old questions and new insights. Science. 2011;332:1519–1523. [PubMed: 21700865]

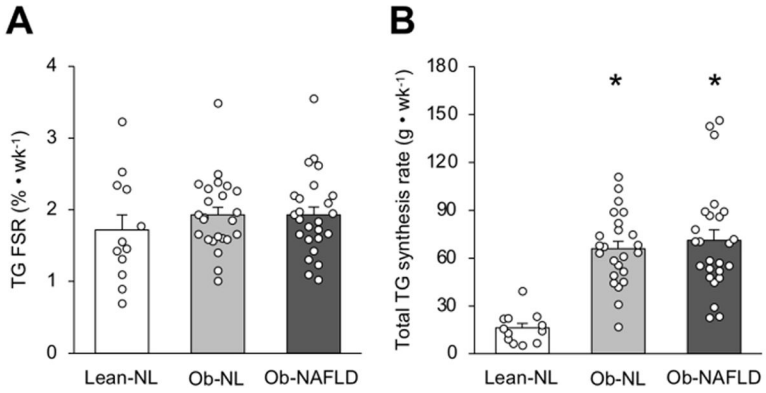

Figure 1. Subcutaneous adipose tissue total lipogenesis is increased in people with obesity.

Fractional **(A)** and total **(B)** triglyceride synthesis rates in subcutaneous abdominal adipose tissue in the Lean-normal (Lean-NL; n=12), Obese-normal (Ob-NL; n=24) and Obese-NAFLD (Ob-NAFLD; n=25) groups. Data are means ± SEM. One-way analysis of variance (ANOVA) and Fisher's least significant difference post-hoc testing used to identify significant mean differences between groups. *P<0.05 *vs.* Lean-NL.

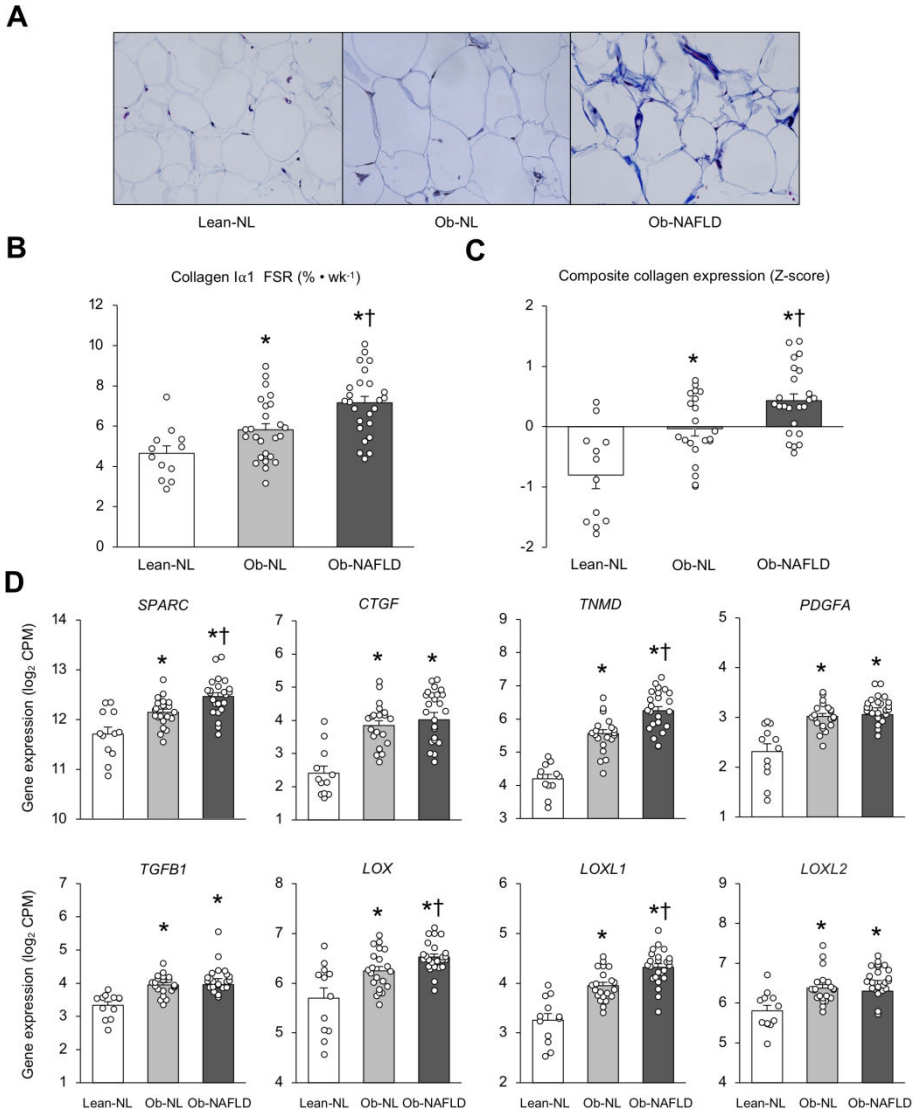

Figure 2. Collagen synthesis rate in subcutaneous adipose tissue is increased in people with obesity and NAFLD.

Masson's trichrome staining of collagen of subcutaneous abdominal adipose tissue from representative Lean-normal (Lean-NL), Obese-normal (Ob-NL) and Obese-NAFLD (Ob-NAFLD) participants (**A**). Collagen Iα1 fractional synthesis rate (**B**), composite collagen gene expression (**C**) and expression of key regulators of extracellular matrix remodeling (**D**) in subcutaneous abdominal adipose tissue in the Lean-normal (Lean-NL; n=12), Obese-normal (Ob-NL; n=25 in panel B, and n=21 in panels C and D) and Obese-NAFLD (Ob-NAFLD; n=25 in panel B, and n=24 in panels C and D) groups. Data are means ± SEM. The composite collagen gene expression values presented in panel C are the average of collagens *1A1, 1A2, 3A1, 5A1, 5A2, 5A3, 6A1, 6A2, 6A3, 12A1, 14A1 and 24A1* after converting expression of each isoform to a *Z*-distribution. One-way analysis of variance (ANOVA) with Fisher's least significant difference post-hoc testing used to identify significant mean differences between groups. *P<0.05 *vs.* Lean-NL. †P<0.05 *vs.* Ob-NL. CPM=counts per million.

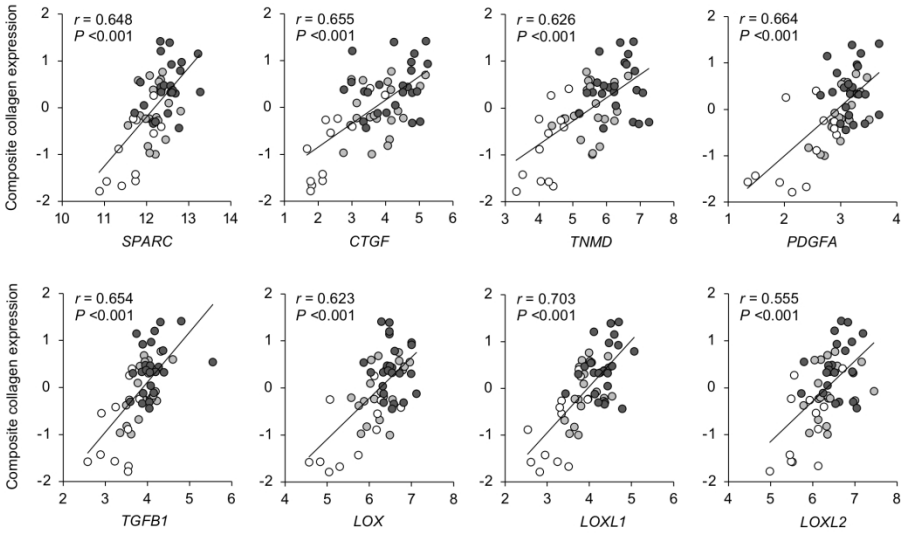

Figure 3. Relationships among adipose tissue expression of genes that regulate extracellular matrix formation and composite collagen gene expression.

Individual data represent Lean-normal (white circles), Obese-normal (gray circles) and Obese-NAFLD (black circles) participants. Linear regression analysis was used to describe the relationship between factors that regulate extracellular matrix formation and composite collagen gene expression.

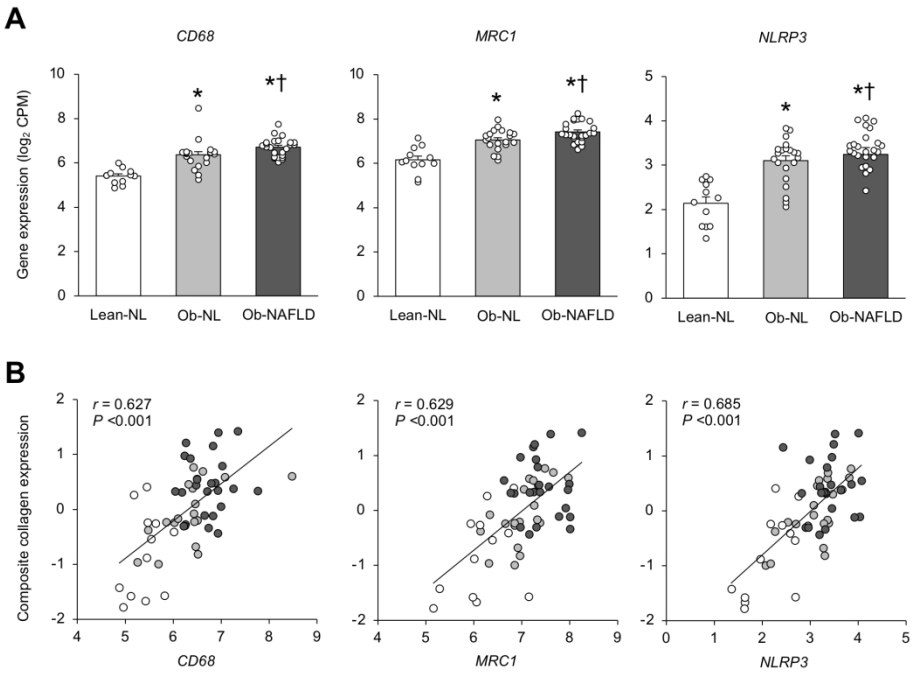

Figure 4. Adipose tissue expression of macrophage markers and the NLRP3 inflammasome and their relationship with collagen gene expression.

Expression of the macrophage markers, cluster of differentiation 68 (*CD68*), and mannose receptor C-type 1 (*MRC1*), and nod-like receptor protein 3 (*NLRP3*) inflammasome (**A**) and their relationships with composite collagen gene expression in subcutaneous abdominal adipose tissue (**B**) in the Lean-normal (Lean-NL; n=12), Obese-normal (Ob-NL; n=21) and Obese-NAFLD (Ob-NAFLD; n=25) groups. Data are means ± SEM in panel A and one-way analysis of variance (ANOVA) and Fisher's least significant difference post-hoc testing used to identify significant mean differences between groups. *P<0.05 *vs.* Lean-NL. †P<0.05 *vs.* Ob-NL. In panel B, Individual data represent Lean-NL (white circles), Ob-NL (gray circles) and Ob-NAFLD (black circles) participants with linear regression analysis used to describe the relationship between factors. CPM=counts per million.

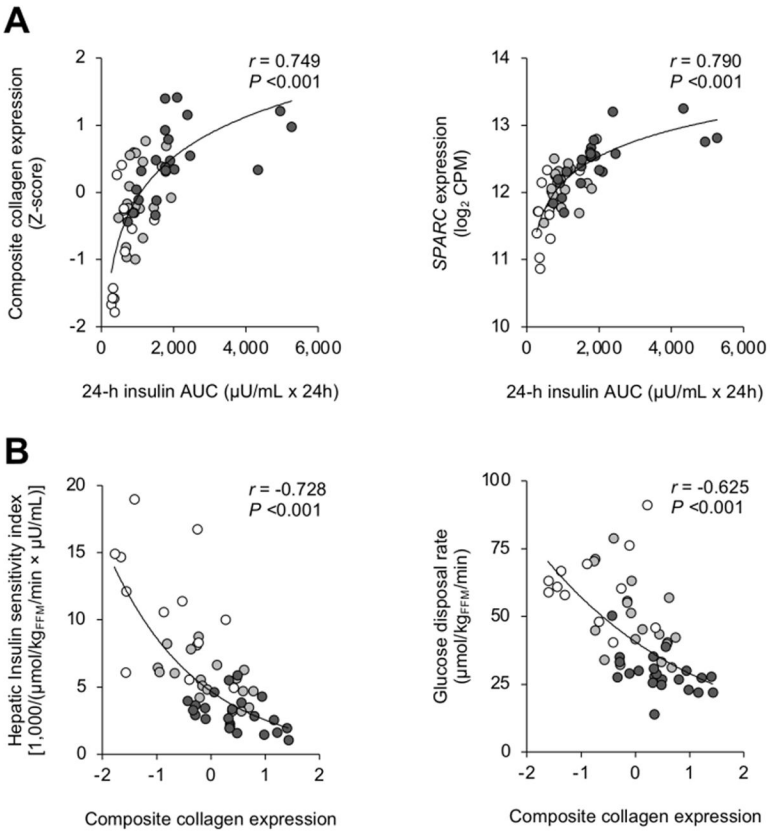

Figure 5. Relationships among 24-h plasma insulin, insulin sensitivity and factors involved in adipose tissue collagen production.

Relationships between subcutaneous adipose tissue (SAT) gene expression of both composite collagen and secreted protein acidic and cysteine rich (*SPARC*) and 24-h plasma insulin concentration area-under-the-curve (AUC) (**A**), and between both SAT composite collagen gene expression and hepatic insulin sensitivity (assessed as the hepatic insulin sensitivity index) and whole-body insulin sensitivity (assessed as the glucose disposal rate during a hyperinsulinemic-euglycemic clamp procedure) (**B**) in Lean-normal (white circles), Obese-normal (gray circles) and Obese-NAFLD (black circles) participants. Non-linear regression analysis was used to determine the relationship between factors.

Table 1.

Body composition and metabolic characteristics of the participants

	Lean-NL (*n*=12)	Ob-NL (*n*=25)	Ob-NAFLD (*n*=25)
Age (y)	38 ± 2	40 ± 1	41 ± 2
Weight (kg)	66.5 ± 1.8	106.0 ± 3.6 *	112.8 ± 3.0 *
BMI (kg/m^2)	23.1 ± 0.5	37.8 ± 1.1 *	39.6 ± 1.1 *
Body fat (%)	29.8 ± 1.8	47.7 ± 1.4 *	48.2 ± 1.5 *
Abdominal SAT volume (cm^3)	1,011 ± 103	3,705 ± 236 *	3,931 ± 246 *
IAAT volume (cm^3)	477 ± 58	1,073 ± 97 *	1,824 ± 114 *†
IHTG content (%)	1.8 ± 0.2	2.6 ± 0.2	17.7 ± 1.6 *†
Fasting insulin (μU/mL)	5.0 ± 0.6	10.7 ± 0.8 *	27.8 ± 3.7 *†
24-h insulin AUC (μU/mL x 24h)[a]	567 ± 96	1,066 ± 76 *	2,044 ± 247 *†
Fasting glucose (mg/dL)	85.9 ± 1.2	87.8 ± 0.9	100.1 ± 2.1 *†
OGTT 2-h glucose (mg/dL)	97.9 ± 5.4	105.9 ± 3.3	167.5 ± 5.4 *†
HbA1c (%)	4.8 ± 0.1	5.0 ± 0.1	5.7 ± 0.1 *†
Triglycerides (mg/dL)	72 ± 9	71 ± 5	146 ± 15 *†
HDL-cholesterol (mg/dL)	64 ± 4	55 ± 3	42 ± 1 *†
LDL-cholesterol (mg/dL)	97 ± 7	101 ± 6	110 ± 6
ALT (U/L)	16 ± 2	17 ± 2	35 ± 8 *†
AST (U/L)	17 ± 1	18 ± 1	25 ± 3 *†
Alkaline Phosphatase (U/L)	56 ± 4	67 ± 4	76 ± 4 *
Bilirubin (mg/dL)	0.49 ± 0.04	0.38 ± 0.03	0.43 ± 0.03
Hepatic insulin sensitivity index [1,000/(μmol/kg$_{FFM}$/min × μU/mL)][b]	11.0 ± 1.2	5.6 ± 0.3 *	3.0 ± 0.3 *†
Glucose disposal rate during the clamp (μmol/kg$_{FFM}$/min)[b]	61.7 ± 4.0	48.6 ± 2.8 *	28.8 ± 1.9 *†

Data are means±SEM. Abbreviations: ALT=alanine aminotransferase; AST=aspartate aminotransferase; AUC=area-under-the-curve; BMI=body mass index; FFM=fat-free mass, HbA1c=hemoglobin A1c; HDL= high-density lipoprotein; IAAT=intraabdominal adipose tissue; IHTG=intrahepatic triglyceride; LDL=low-density lipoprotein; NL=normal IHTG content and oral glucose tolerance; Ob=obese; OGTT=oral glucose tolerance test; SAT=subcutaneous adipose tissue.

[a] Lean-NL n=12; Ob-NL n=24; Ob-NAFLD n=24.

[b] Lean-NL n=12; Ob-NL n=23; Ob-NAFLD n=24. One-way analysis of variance (ANOVA) with Fisher's least significant difference post-hoc testing where appropriate were used to identify significant mean differences between groups.

* $P<0.05$ *vs.* Lean-NL.

† $P<0.05$ *vs.* Ob-NL.